

# Tropical Fermat-Weber Polytopes

John Sabol

David Barnhill

Ruriko Yoshida

Keiji Miura

## Abstract

We study the geometry of tropical Fermat-Weber points in terms of the symmetric tropical metric over the tropical projective torus. It is well-known that a tropical Fermat-Weber point of a given sample is not unique and we show that the set of all possible Fermat-Weber points forms a polytrope. To prove this, we show that the tropical Fermat-Weber polytrope is a bounded cell of a tropical hyperplane arrangement given by both max- and min-tropical hyperplanes with apices given by the sample. We also define tropical Fermat-Weber gradients and provide a gradient descent algorithm that converges to the Fermat-Weber polytrope.

## 1 Introduction

Consider a sample  $\mathcal{S} := \{p_1, \dots, p_n\}$ , and suppose we wish to find a point  $x$  that minimizes the sum of distances from  $x$  to all points in  $\mathcal{S}$  with respect to the distance metric  $\mathbf{d}$ . This problem is known as the *Fermat-Weber location problem*. Since Weiszfeld in [20], there has been much work done with an Euclidean metric (for example, see [4] and references within). This optimal point  $x^*$  is called a *Fermat-Weber point* of the sample  $\mathcal{S}$ , and it is defined as

$$x^* = \arg \min_x \sum_{i=1}^n \mathbf{d}(x, p_i).$$

Fermat-Weber points are a form of geometric median which describe central tendency in data and which, like their one-dimensional counterparts, are robust against outliers. They have many applications in statistical analysis and optimization, particularly in the area of phylogenetics. For example, Huggins et al. in [12] used Fermat-Weber points to define a Bayes estimator for a phylogenetic tree reconstruction given an alignment as the minimizer of the expected loss, while Comănesci and Joswig in [6] showed a correspondence between Fermat-Weber points and optimal solutions of a transportation problem to compute consensus trees. Recently Comănesci in [5] defined tropically quasiconvex functions and applied them to compute asymmetric tropical Fermat-Weber points.

In this paper we consider Fermat-Weber points over the tropical projective torus,  $\mathbb{R}^d/\mathbb{R}\mathbf{1}$ , using the *tropical metric*  $d_{\text{tr}}$  and call these points *tropical Fermat-Weber points*. Here we note that for our paper  $d_{\text{tr}}$  refers to the *symmetric* metric, which distinguishes it from the *asymmetric* metric considered by Comănesci and Joswig in [6]. Details on the equivalence relation for the quotient defining  $\mathbb{R}^d/\mathbb{R}\mathbf{1}$  and the definition of  $d_{\text{tr}}$  are provided in Section 2. It is well known that a tropical Fermat-Weber point of a given sample  $\mathcal{S} \subset \mathbb{R}^d/\mathbb{R}\mathbf{1}$  is not generally unique, and in 2017 Lin et al. proposed a method for finding the set of tropical Fermat-Weber points, which we denote  $FW(\mathcal{S})$ , as optimal solutions to a linear program [16]. Later in [17], Lin and Yoshida studied the geometry of this set, proving that  $FW(\mathcal{S})$  defines a classically convex polytope in  $\mathbb{R}^{d-1}$  (which is isomorphic to  $\mathbb{R}^d/\mathbb{R}\mathbf{1}$ ) and providing conditions for which  $FW(\mathcal{S})$  is a singleton.

Thus, our object of interest is the polytope defined by the set of tropical Fermat-Weber points of a given sample. More precisely we consider the set

$$FW(\mathcal{S}) := \left\{ x^* \in \mathbb{R}^d/\mathbb{R}\mathbf{1} \mid x^* = \arg \min_x \sum_{i=1}^n d_{\text{tr}}(x, p_i) \right\} \quad (1)$$

for  $\mathcal{S} := \{p_1, \dots, p_n\} \subset \mathbb{R}^d/\mathbb{R}\mathbf{1}$ . Our main contribution is that  $FW(\mathcal{S})$  is tropically convex over  $\mathbb{R}^{d-1} \cong \mathbb{R}^d/\mathbb{R}\mathbf{1}$ . This means that the polytope defined by the set of tropical Fermat-Weber points of a sample  $\mathcal{S}$  is a *polytrope* in  $\mathbb{R}^{d-1} \cong \mathbb{R}^d/\mathbb{R}\mathbf{1}$  since  $FW(\mathcal{S})$  is known to be classically convex [17]. Additional contributions of this research are as follows:

- We introduce a dual program to the one proposed in [16], providing an intuitive geometric interpretation and connection to several concepts in the literature.

- We prove that  $FW(\mathcal{S})$  is a bounded cell of the union of max-plus and min-plus *covector decompositions* generated by max- and min-plus *tropical hyperplane arrangements* each defined by the set of tropical hyperplanes with apices  $\{p_1, \dots, p_n\}$ . Therefore  $FW(\mathcal{S})$  is a polytrope.
- We provide a precise definition and formula for *tropical Fermat-Weber gradients* and *subdifferentials*, proving that  $x^*$  is a Fermat-Weber point if and only if zero is an element of its tropical Fermat-Weber subdifferential.
- We introduce a *tropical Fermat-Weber gradient descent* algorithm that converges towards  $FW(\mathcal{S})$  for any  $x \in \mathbb{R}^d/\mathbb{R}\mathbf{1}$ .

## 2 Tropical Basics

Here we establish notations, definitions, and some required facts to support our methods while briefly reminding readers of some basics from tropical geometry. For details, we refer to [14].

### 2.1 Tropical Building Blocks

**Definition 1** (Tropical Semiring). *Over the tropical semiring  $\mathbb{T}_{max} := (\mathbb{R} \cup \{-\infty\}, \oplus, \odot)$ , tropical addition ( $\oplus$ ) and multiplication ( $\odot$ ) are defined as  $a \oplus b := \max\{a, b\}$  and  $a \odot b := a + b$  where  $a, b \in \mathbb{R} \cup \{-\infty\}$ .*

This semiring has  $-\infty$  as the identity element under addition, i.e.,  $a \oplus -\infty = a$  for any  $a \in \mathbb{R}$ , and 0 as the identity element under multiplication. Extension to scalar multiplication and vector addition through componentwise application yields the *tropical semimodule*  $(\mathbb{T}_{max}^d, \oplus, \odot)$ .

Throughout this paper we will frequently use  $\mathbb{T}_{max}$  and  $\mathbb{T}_{max}^d$  to denote elements in  $\mathbb{R} \cup \{-\infty\}$  and  $(\mathbb{R} \cup \{-\infty\})^d$ , sometimes dropping the *max* subscript when the meaning is clear from context. While we define our semiring here using the *max-plus* algebra, there is a corresponding *min-plus* version denoted by  $\mathbb{T}_{min}$  with elements in  $\mathbb{R} \cup \{+\infty\}$ , where  $a \oplus b := \min\{a, b\}$ , and with  $\infty$  as the additive identity. The isomorphism between *max-plus* and *min-plus* semirings is reflective around the origin, demonstrated by the equality  $\max\{x, y\} = -\min\{-x, -y\}$ . Since our paper frequently leverages both *max* and *min* concepts simultaneously, we will endeavor to specify which version is intended where such distinctions are necessary.

**Definition 2** (Tropical Projective Space and Tropical Projective Torus). *The tropical projective space  $\mathbb{TP}^{d-1} = (\mathbb{T}^d \setminus \{-\infty\mathbf{1}\})/\mathbb{R}\mathbf{1}$  is a quotient vector space modulo the subspace generated by the span of the all-ones vector  $\mathbf{1} := (1, \dots, 1)$ . The tropical projective torus  $\mathbb{R}^d/\mathbb{R}\mathbf{1}$  is the subset of points in  $\mathbb{TP}^{d-1}$  with finite coordinates.*

The tropical projective torus is homeomorphic to  $\mathbb{R}^{d-1}$  via the bijective map

$$(x_1, \dots, x_d) + \mathbb{R}\mathbf{1} = (0, x_2 - x_1, \dots, x_d - x_1) + \mathbb{R}\mathbf{1} \mapsto (0, x_2 - x_1, \dots, x_d - x_1). \quad (2)$$

In general this mapping is not unique, and we set  $x_1 = 0$  (as above) as our convention throughout. This choice is in slight contrast with the *canonical projection* which projects uniquely into the non-negative orthant so that at least one coordinate of  $x$  is zero. Later on, as a technicality, we will work primarily in the tropical projective torus  $\mathbb{R}^d/\mathbb{R}\mathbf{1}$  rather the tropical projective space  $\mathbb{TP}^{d-1}$ , wherein one can assume all points have finite coordinates.

**Definition 3** (Tropical Cones). *A tropical cone in the tropical semimodule  $\mathbb{T}^d$  is a subsemimodule given by*

$$\text{tpos}(M) = \{\lambda_1 \odot p_1 \oplus \dots \oplus \lambda_n \odot p_n \mid \lambda_i \in \mathbb{T}, p_i \in M\}, \quad (3)$$

where  $M$  defines a set of generators. Such a cone is called *polyhedral* if it is finitely generated.

Since every tropical cone contains the point  $-\infty\mathbf{1}$ , the set in (3) is always non-empty. A subset of  $\mathbb{TP}^{d-1}$  is *tropically convex* if it arises as the image of a tropical cone in  $\mathbb{T}^d$  under canonical projection.

**Definition 4** (Tropical Polytopes). *A tropical polytope  $\mathcal{P}$  is the tropical convex hull (tconv) of finitely many points, where for  $V = \{v_1, \dots, v_n\} \subset \mathbb{TP}^{d-1}$  we define*

$$\text{tconv}(V) = \{a_1 \odot v_1 \oplus \dots \oplus a_n \odot v_n \mid a_1, \dots, a_n \in \mathbb{R}\} \quad (4)$$

to be the smallest tropically convex subset of  $V$  containing  $V$ .

Tropical polytopes are tropically convex sets, which means that for any  $a, b \in \mathbb{R}$  and for any  $u, v \in \mathcal{P}$  we have  $a \odot u \oplus b \odot v \in \mathcal{P}$ . A set which is tropically convex in terms of *max-plus* is not (in general) tropically convex in terms of *min-plus*. When a set does happen to be tropically convex in both conventions we call it *bi-tropically convex*. It is easy to show that classical convexity is a natural byproduct of bi-tropical convexity [14] but that the converse does not hold. Since we earlier defined a *polytrope* to be a set that is both classically and tropically convex, we now also see that bi-tropical convexity is a sufficient condition for a polytrope.

**Definition 5** (Generalized Hilbert Projective Metric). *For any points  $u := (u_1, \dots, u_d), v := (v_1, \dots, v_d) \in \mathbb{R}^d/\mathbb{R}\mathbf{1}$ , the tropical distance, or tropical metric,  $d_{\text{tr}}$  between  $u$  and  $v$  is defined as:*

$$d_{\text{tr}}(u, v) := \max_{i \in [d]} \{u_i - v_i\} - \min_{i \in [d]} \{u_i - v_i\}. \quad (5)$$

Note that Equation (5) is equivalently defined regardless of whether one is operating in the *max-plus* or *min-plus* semiring, hence its characterization as a *symmetric* metric.

With our tropical metric, it is natural to consider a *tropical ball*, which is analogous to its Euclidean counterpart but with its radius measured using the tropical metric.

**Definition 6** (Tropical Ball [8]). *For a given point  $\omega \in \mathbb{R}^d/\mathbb{R}\mathbf{1}$ , and a radius  $r > 0$ , a tropical ball, denoted as  $\mathcal{B}_r(\omega)$ , is defined*

$$\mathcal{B}_r(\omega) = \{x \in \mathbb{R}^d/\mathbb{R}\mathbf{1} \mid d_{\text{tr}}(\omega, x) \leq r\}. \quad (6)$$

Each tropical ball,  $\mathcal{B}_r(\omega)$  represents a translation and scaling of a tropical unit ball  $\mathcal{B}_1(\mathbf{0})$ : a tropical ball with radius equal to one and center at the origin. In general, tropical balls possess a well-defined structure. The fact that  $\mathcal{B}_r(\omega)$  is generated as  $\text{tconv}(V')$  by a minimal set of vertices  $V'$  of cardinality  $d$  makes it a tropical simplex in the sense of [15]. For general vertices that may or may not be generators, we use the term *pseudo-vertices* which are the vertices of the polyhedral decomposition defined in [9]. Every tropical ball has  $|V| = 2^d - 2$  pseudo-vertices and  $d(d-1)$  facets. Tropical balls are zonotopes as well as polytropes. Figure 1 (left) shows the tropical ball  $\mathcal{B}_r(\omega)$  with vertices of the max-plus generating set filled black and remaining pseudo-vertices filled white. Tropical balls have a direct structural connection to tropical hyperplanes and tropical sectors, which we shall see in a moment.

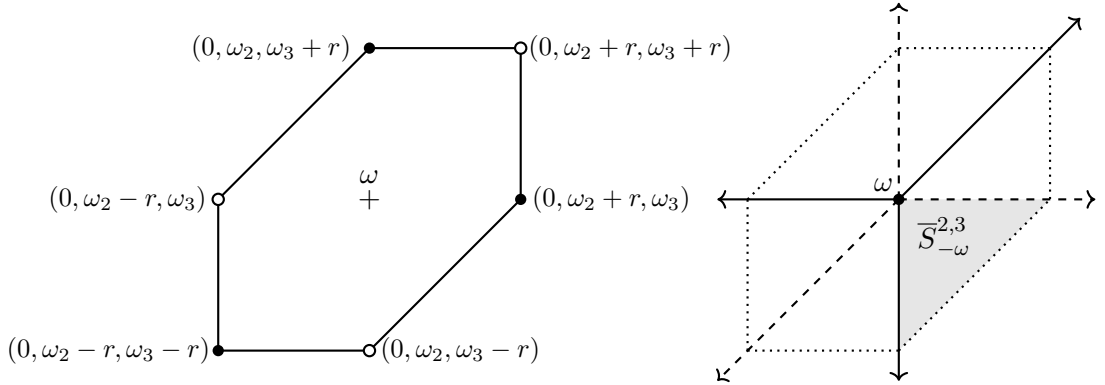


Figure 1: Left: Tropical ball,  $\mathcal{B}_r(\omega) \in \mathbb{R}^3/\mathbb{R}\mathbf{1}$  with radius  $r$ . Center point is indicated by “+” and the minimum generating set  $V'$  are shown as black closed circles. Pseudo-vertices not part of  $V'$  are shown as open circles. Right: The max-plus (solid) and min-plus (dashed) tropical hyperplanes with apex at  $\omega$ , along with  $\mathcal{B}_r(\omega)$  (dotted). Note the correspondence between the rays of the min-plus hyperplane and the generating vertices of  $\mathcal{B}_r(\omega)$ .  $\bar{S}_\omega^{2,3} := \bar{S}_\omega^{\text{max},2} \cap \bar{S}_\omega^{\text{min},3}$  (grey) shows the intersection of the  $2^{\text{nd}}$  closed sector of  $\mathcal{H}_\omega^{\text{max}}$  with the  $3^{\text{rd}}$  closed sector of  $\mathcal{H}_\omega^{\text{min}}$ .

**Definition 7** (Tropical Hyperplanes [14]). *Given some vector  $\nu := (\nu_1, \dots, \nu_d) \in \mathbb{T}_{\text{max}}^d$  with a support that contains at least two elements ( $\#\text{supp}(\nu) \geq 2$ ), the max-tropical hyperplane  $\mathcal{H}_\nu^{\text{max}}$  is the set of points  $x \in \mathbb{TP}^{d-1}$  such that*

$$\max_{i \in [d]} \{x_i + \nu_i\} \quad (7)$$

*is attained at least twice.*

A min-tropical hyperplane  $\mathcal{H}_\nu^{\min}$  can be equivalently defined on  $\mathbb{T}_{min}^d$  with *max* replacing *min* in (7) so that anything presented in terms of max-plus has a min-plus counterpart in the corresponding semiring.  $\nu$  is the normal vector of  $\mathcal{H}_\nu^{\max}$  with  $\omega := -\nu$  being the *apex* of  $\mathcal{H}_\nu^{\max}$ . The requirement on the support of  $\nu$  in (7) ensures that the hyperplane is non-empty. As with tropical balls, any  $\mathcal{H}_\nu^{\max}$  can be viewed as a translation of  $\mathcal{H}_0^{\max}$ , the tropical hyperplane with apex at the origin [13, Proposition 2.6]. In Figure 1 (right), we see  $\mathcal{H}_{-\omega}^{\max}$  (solid lines) superimposed with  $\mathcal{H}_{-\omega}^{\min}$  (dashed lines), with each hyperplane individually partitioning  $\mathbb{R}^d/\mathbb{R}\mathbf{1}$  into exactly  $d$  sectors.

**Definition 8** (Tropical Sectors from Section 5.5 in [14]). *For  $i \in [d]$ , the  $i$ -th closed sector of  $\mathcal{H}_\nu^{\max}$  is defined as*

$$\bar{S}_\nu^{\max,i} := \bigcap_{j \in \text{supp}(\nu)} \{x \in \mathbb{R}^d \mid \nu_i + x_i \geq \nu_j + x_j\}. \quad (8)$$

When the inequality in (8) is strict, we call it the  $i$ -th *open sector* of  $\mathcal{H}_\nu^{\max}$  and write  $S_\nu^{\max,i}$ . Closed sectors are the topological closure of open sectors. Every closed sector of a tropical hyperplane is a tropical cone with respect to both max and min, implying that their projections to the tropical projective torus are bi-tropically (and classically) convex [14]. Equation (8) shows that each sector corresponds to the intersection of  $d - 1$  Euclidean half-spaces. In particular, they are weighted digraph polyhedra as defined in [14], and their unions form *tropical halfspaces* [13]. As depicted in Figure 1, the closed sectors of a tropical hyperplane given by  $\nu$  generate a polyhedral decomposition of  $\mathbb{R}^d/\mathbb{R}\mathbf{1}$  called the *normal complex*  $\text{NC}(\nu)$ . See [14] for details. Sectors correspond to indices of maximal (resp. minimal) elements of their normal vector. That is, for  $x \in \mathbb{R}^d/\mathbb{R}\mathbf{1}$ , we can conveniently rephrase  $\text{argmax } x = \{i\}$  as  $x \in \bar{S}_0^{\max,i}$  and equivalently,  $\text{argmin } x = \{j\}$  as  $x \in \bar{S}_0^{\min,j}$ . Given  $\omega$  with full support, one can write

$$\bar{S}_{-\omega}^{\min,i} = \omega + \bar{S}_0^{\min,i} \quad \text{and} \quad \bar{S}_{-\omega}^{\max,i} = \omega + \bar{S}_0^{\max,i}, \quad (9)$$

where for notational convenience we will sometimes drop  $\mathbf{0}$ . Thus, for  $x, \omega \in \mathbb{R}^d/\mathbb{R}\mathbf{1}$  we have

$$x \in \bar{S}_{-\omega}^{\max,i} \iff i \in \text{argmax}\{x - \omega\} \iff \omega \in \bar{S}_{-x}^{\min,i}. \quad (10)$$

## 2.2 Tropical Configurations

We now transition to consider collections of points  $\mathcal{S} = \{p_1, \dots, p_n\} \subset \mathbb{TP}^{d-1}$ , which we will sometimes associate to the  $n \times d$ -matrix  $V$  with coefficients  $v_{ij}$  in  $\mathbb{T}$ . Each row of  $V$  corresponds to a point from  $\mathcal{S}$ , and we use both notations interchangeably. As a general rule, we write  $v_i$  as row vectors and  $v^{(j)}$  for column vectors of  $V$  when such distinctions are required.

**Definition 9** (Tropical Hyperplane Arrangement from Section 4.5 in [14]). *For  $\mathcal{S} = \{p_1, \dots, p_n\} \subset \mathbb{TP}^{d-1}$ , the tropical hyperplane arrangement given by  $\mathcal{T}^{\max}(\mathcal{S})$  is the union of  $n$  tropical hyperplanes with apices  $-p_i$  for all  $i \in [n]$ . That is,*

$$\mathcal{T}^{\max}(\mathcal{S}) := \mathcal{H}_{-p_1}^{\max} \cup \dots \cup \mathcal{H}_{-p_n}^{\max}, \quad (11)$$

and we say that the arrangement has full support if  $V$  has only finite coefficients.

Recall how each hyperplane generates a normal complex that decomposes  $\mathbb{R}^d/\mathbb{R}\mathbf{1}$  into non-empty closed sectors. Then for a union of several hyperplanes (i.e. a hyperplane arrangement) we get a common refinement of the normal complex called the *covector decomposition* of  $V$ , or  $\text{CovDec}(V)$ .

**Definition 10** (Covector Decomposition from Section 6.3 in [14]). *The covector decomposition induced by  $V$  is a polyhedral subdivision of  $\mathbb{R}^d/\mathbb{R}\mathbf{1}$  generated by the tropical hyperplane arrangement  $\mathcal{T}(V)$ .*

The cells of this subdivision, called *covector cells*, may be bounded or unbounded and are bi-tropically convex [14]. Ardila and Develin first showed in [2] that this subdivision is combinatorially isomorphic to the complex of interior faces of the regular subdivision of a product of simplices, and provided a definition for the “type” of a point  $x \in \mathbb{TP}^{d-1}$  given such an arrangement. These *types* encode the combinatorial structure of a tropical hyperplane arrangement  $\mathcal{T}(V)$  as an  $n$ -tuple where the  $i$ -th element corresponds to the set of closed sectors in  $\mathcal{H}_{-v_i}$  that contain  $x$ . Since sector inclusion changes only when  $x$  crosses a face of a hyperplane in  $\mathcal{T}$ , all points within a common face are of the same type.

Of course, one can similarly encode the same combinatorial structure via a  $d$ -tuple whose  $j$ -th element records the indices for the set of points  $v_i \in V$  whose  $i$ -th closed sector contains  $x$ . We follow [14] and call this a *covector*. Covectors, which are tuples (not vectors), correspond to cells in  $\text{CovDec}(V)$  in the same way that types correspond to faces in  $\mathcal{T}(V)$ .

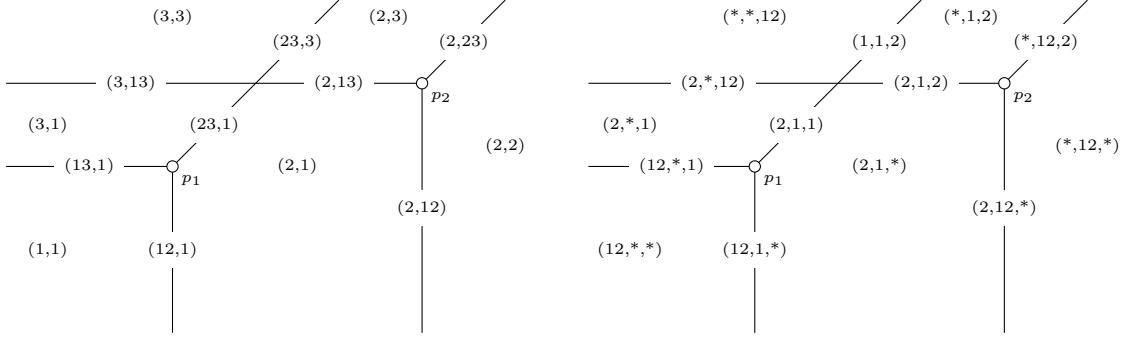


Figure 2: Left: Tuples defining the “type” for each face of the hyperplane arrangement given by  $\mathcal{S}$  in Example 1. Not shown are types for the 0-dimensional faces  $p_1$ ,  $p_2$ , and  $(0, 1, 1)$  (the intersection of hyperplanes), but they can be easily inferred. For instance, the point  $(0,1,1)$  has type  $(23, 13)$ . Right: Covectors corresponding to the cells of  $CovDec(V)$ , where a “\*” denotes the empty set. Again, covectors for 0-dimensional cells are not shown.

**Definition 11** (Tropical Types from [2] and Covectors from [14]). *For a point  $x \in \mathbb{R}^d/\mathbb{R}\mathbf{1}$  and a tropical hyperplane arrangement given by a  $n \times d$  matrix  $V$  with coefficients in  $\mathbb{T}^{max}$ , the type of a face of  $\mathcal{T}^{max}(V)$  containing  $x$  is an  $n$ -tuple given by  $t(x, V) = (t_1, \dots, t_n)$  where each element  $t_i \subseteq [d]$  encodes the set of closed sectors of  $\mathcal{H}_{-v_i}^{max}$  containing  $x$ . The covector of a cell of  $CovDec(V)$  is a  $d$ -tuple  $\tau(x, V) = (\tau_1, \dots, \tau_d)$  where each element  $\tau_j \subset [n]$  encodes the subset of points in  $V$  for which  $x$  is an element of the  $j$ -th closed sector.*

$$t_i := \left\{ j \in [d] \mid x \in v_i + \overline{S}^{max,j} \right\} \quad i = 1, \dots, n \quad \text{Tropical Type} \quad (12)$$

$$\tau_j := \left\{ i \in [n] \mid x \in v_i + \overline{S}^{max,j} \right\} \quad j = 1, \dots, d \quad \text{Covector} \quad (13)$$

**Example 1.** *Consider two points in  $\mathbb{R}^d/\mathbb{R}\mathbf{1}$  given by  $\mathcal{S} = \{p_1, p_2\} = \{(0, 0, 0), (0, 3, 1)\}$ , and see Figure 2 for a depiction of the types and covectors for various points in  $CovDec(\mathcal{S})$ .*

It is often convenient to encode a type tuple or a covector as a matrix. We do so with a 0/1-matrix of dimension  $n \times d$  where each row corresponds to the  $i$ -th tropical hyperplane in  $\mathcal{T}(V)$ , and each column to its  $j$ -th sector. Such matrices are called the “fine-type” of a point  $x \in \mathbb{R}^d/\mathbb{R}\mathbf{1}$  [14].

**Definition 12** (Fine-Type Matrices from [10]). *For  $x, V$  as in Definition 11, the fine-type of  $x$  is the 0/1-matrix  $T$  of dimension  $n \times d$  where*

$$T(x, V) = (T_{ij}) := \begin{cases} 1 & x \in v_i + \overline{S}^{max,j} \\ 0 & \text{otherwise.} \end{cases} \quad (14)$$

*The transpose of the fine-type matrix is called the dual fine-type.*

Regardless of whether one prefers to work with the fine-type or dual fine-type, it is natural to consider the row and column sums of such a matrix, and to this end, we discuss the “coarse-types” [14] of a point  $x$  as follows.

**Definition 13** (Coarse-Types from [10]). *For  $x, V$  as in Definition 11, the coarse-type of  $x$  is a vector of length  $d$  corresponding to the column sums of the fine-type matrix  $T$ . Similarly, the dual coarse-type of  $x$  is a vector of length  $n$  corresponding to the column sums of the dual fine-type matrix, or equivalently, the row sums of  $T$ .*

$$\#t_i(x, V) := \sum_j T_{ij} \quad i = 1, \dots, n \quad \text{Dual Coarse-Type} \quad (15)$$

$$\#\tau_j(x, V) := \sum_i T_{ij} \quad j = 1, \dots, d \quad \text{Coarse-Type} \quad (16)$$

*Dual coarse-type can be equivalently defined by the element-wise cardinality of the type tuple, and likewise, coarse-types by the cardinality of elements of the covector tuple.*

As a 0/1-matrix, fine-types encode the adjacency of nodes in a particular bi-partite directed graph. To see how, consider the complete bipartite graph  $K_{n,d}$  with  $[n] \sqcup [d]$  nodes and from it generate a

subgraph by keeping only arcs  $(i, j)$  where  $j \in t_i$  (or equivalently, where  $i \in \tau_j$ ) for any particular type/covector. The resulting  $n \times d$  bipartite graph is called the *covector graph*, which we denote  $\mathcal{G}$ . In this way, a fine-type matrix is the adjacency matrix of its covector graph. Every minimal (with respect to inclusion) cell in  $\text{CovDec}(V)$  can be uniquely represented by its corresponding covector graph, which is a unique maximal subgraph of  $K_{n,d}$  [14]. The next example will help to tie these definitions together.

**Example 2.** Consider the sample  $\mathcal{S} := \{(0, 0, 1), (0, 2, 5), (0, 3, 2)\} \subset \mathbb{TP}^2$  and let  $C$  be the unique bounded and closed cell in  $\text{CovDec}(\mathcal{S})$  as shown in Figure 3. By considering which sectors of the hyperplane arrangement contain  $C$ , we can determine the fine-type matrix  $T$  and its associated covector graph  $\mathcal{G}_C$ . Note in particular how the bipartite graph  $\mathcal{G}_C$  encodes the type and covector by the degree of each of its nodes.

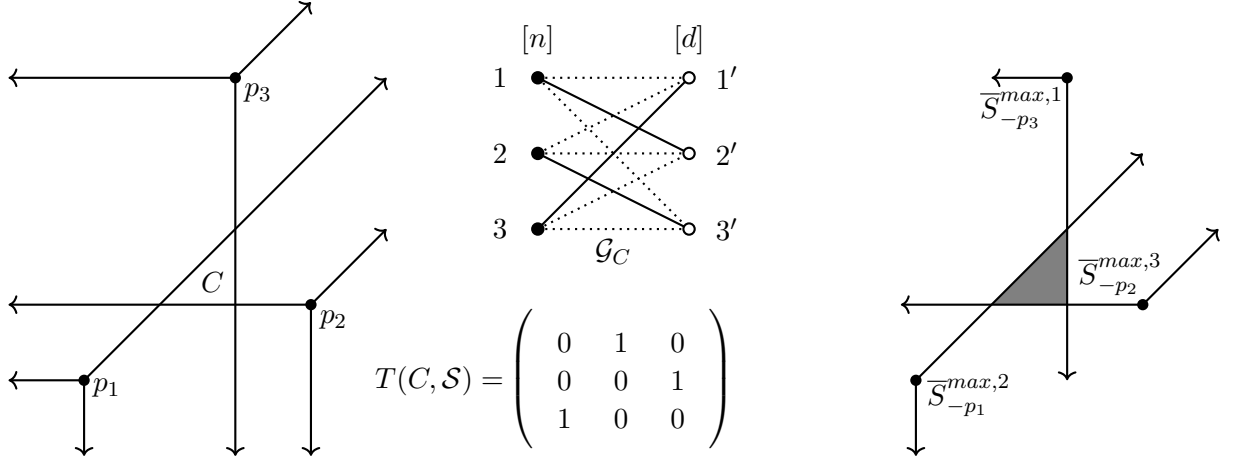


Figure 3: Left:  $\text{CovDec}(\mathcal{S})$  with the unique bounded cell  $C$ . Center: The bipartite graph  $K_{n,d}$  (dotted arcs) overlaid by its subgraph  $\mathcal{G}_C$  (solid arcs), the covector graph of cell  $C$ .  $\mathcal{G}_C$  encodes the combinatorial structure of the hyperplane arrangement  $\mathcal{T}(\mathcal{S})$ , which is equivalently represented by the fine-type matrix  $T$  shown below the graph. The dual coarse-type  $\#t = (1, 1, 1)$  is equal to the coarse-type  $\#\tau$  in this instance. Right: The intersection (shaded grey) of the three cones defined by the covector graph and fine-type matrix, which reconstructs  $C$ .

Since fine-types and covectors are the same for any point within a closed cell  $C$ , we will sometimes denote these as a function of the cell (i.e.,  $T(C, V)$ ,  $\tau(C, V)$ ) rather than as a function of a particular point  $x \in C$  based on whatever is most convenient. For Example 2, the type is given by  $t(C, \mathcal{S}) = (2, 3, 1)$  and the covector is given by  $\tau(C, \mathcal{S}) = (3, 1, 2)$ . We will similarly alternate notation for covector graphs by sometimes referencing them in relation to a point  $x$  as in  $\mathcal{G}(x)$ , to a covector as in  $\mathcal{G}(\tau)$ , or to a cell as in  $\mathcal{G}(C)$ , believing that the meaning will be clear in such contexts. When we refer to  $\mathcal{G}(x)$  it is assumed that we mean the minimal (with respect to inclusion) cell containing  $x$ .

## 2.3 Max and Min Together

Up to this point we have operated on a single version (either max or min) of the tropical semiring. We now wish to operate on both concurrently. That is, we wish to employ max-plus and min-plus concepts together. This requires that we work in the tropical projective torus  $\mathbb{R}^d/\mathbb{R}\mathbf{1}$ , which works for both max and min simultaneously. Thus, moving forward we assume that all points  $p \in \mathcal{S}$  have full support, and equivalently, all entries in  $V$  are finite.

To prepare the way for this merger, we update our notation as follows. Max-plus objects will retain our original notation, as in  $\tau$ ,  $\#t$ ,  $\#\tau$ , and  $T$  for covectors, coarse types, dual coarse types, and fine-type matrices respectively. For objects derived using min-plus algebra we add an overhead bar, as in  $\bar{\tau}$ ,  $\#\bar{t}$ ,  $\#\bar{\tau}$ , and  $\bar{T}$ . Covector graphs may use  $\mathcal{G}(\tau)$  or  $\mathcal{G}(\bar{\tau})$  if the associated covector is apparent, or  $\mathcal{G}_x^{max}$ ,  $\mathcal{G}_x^{min}$  for a point/cell if distinction is necessary.

**Definition 14** (Tropical Half-Sectors). An open tropical half-sector is the nonempty intersection of an open max-plus sector with that of an open min-plus sector, both with apex  $\omega$ , i.e.,

$$S_{-\omega}^{i,j} := S_{-\omega}^{max,i} \cap S_{-\omega}^{min,j}, \quad (17)$$

where  $i, j \in [d]$  index the max/min-plus hyperplane sectors respectively.

From the definition, it is straightforward to see that if  $i = j$  then no such intersection is possible. Thus, our definition of tropical half-sectors *implies*  $i \neq j$  even when considering their topological closure, which form *closed* tropical half-sectors in the same sense as Definition 8. For our purposes, we are interested the latter so that one may safely assume future references are with regard to closed half-sectors unless otherwise noted.

Figure 1 (right) depicts the half-sector generated by the second sector of a max-plus hyperplane intersected and the third sector of a min-plus hyperplane. Recall that each sector of a tropical hyperplane is a weighted digraph polyhedron. Since intersections of weighted digraph polyhedra are again weighted digraph polyhedra [14], it follows that tropical half-sectors are also weighted digraph polyhedron. Viewed as translates from the origin, tropical half-sectors are also polyhedral cones, which leads to the following definition.

**Definition 15** (Face Fan of  $\mathcal{B}(\mathbf{0})$ ). *Let  $\mathcal{F}$  be the polyhedral fan generated by the set of all closed half-sectors, i.e.,*

$$\mathcal{F} := \{ \bar{S}_0^{i,j} \mid i, j \in [d] \}, \quad (18)$$

which we call the face fan of the tropical ball  $\mathcal{B}(\mathbf{0})$ .

In general, the face fan of a polytope  $\mathcal{P}$  is the set of all cones spanned by proper faces of  $\mathcal{P}$  [21]. That is to say, each  $\bar{S}^{i,j}$  defines a cone that is facet-defining for  $\mathcal{B}(\mathbf{0})$ . Thus,  $\mathcal{F}$  has cardinality  $|\mathcal{F}| = d(d-1)$  and each cone in  $\mathcal{F}$  corresponds to the indices of the maximal and minimal elements of  $x \in \mathbb{R}^d/\mathbb{R}\mathbf{1}$ . Since  $\mathcal{F}$  encodes only the maximal and minimal indices, rather than a complete ordering on  $[d]$ , we can view  $\mathcal{F}$  as a coarsening of the *braid arrangement*.

We again consider a translation of the tropical ball from its center at the origin, to some general point  $\omega \in \mathbb{R}^d/\mathbb{R}\mathbf{1}$ , and admit a slight abuse of terminology by calling  $\mathcal{F}(\omega) := \mathcal{F} + \omega$  the *face fan* of  $\mathcal{B}(\omega)$ . Viewed as a hyperplane arrangement,  $\mathcal{F}(\omega)$  provides a common refinement of  $\mathbb{R}^d/\mathbb{R}\mathbf{1}$  in the manner one would expect, i.e., as the union of normal complexes corresponding to both max- and min-plus hyperplanes. More precisely,

$$\mathcal{F}(\omega) := \mathcal{H}_{-\omega}^{\max} \cup \mathcal{H}_{-\omega}^{\min} = \mathcal{H}_{-\omega}^{\max} \cup -\mathcal{H}_{-\omega}^{\max}, \quad (19)$$

which decomposes  $\mathbb{R}^d/\mathbb{R}\mathbf{1}$  into  $d(d-1)$  cells of maximum dimension [14]. If we consider a collection of points each representing an apex for  $\mathcal{F}$  we arrive at a bi-tropical version of the covector decomposition.

**Definition 16** (Bi-Tropical Covector Decomposition). *For an  $n \times d$ -matrix  $V$  with finite coefficients  $v_{ij}$ , the bi-tropical covector decomposition induced by  $V$ , denoted  $BCD(V)$ , is the common refinement of  $\mathbb{R}^d/\mathbb{R}\mathbf{1}$  generated by the union of max-plus and min-plus hyperplanes each with apices at  $v_i$  for all  $i = 1, \dots, n$ . It is precisely the union of covector decompositions generated by each version of the tropical semiring.*

Each cell  $C$  in  $BCD(V)$  corresponds to a unique pair of max-plus and min-plus covectors, along with their associated covector graphs and fine-type matrices. As intersections of tropical cones, these cells remain bi-tropically convex. We can write them as

$$C(\tau, \bar{\tau}) = \left\{ x \in \mathbb{R}^d \mid \begin{array}{l} x_j - x_{j'} \geq v_{ij} - v_{ij'} \quad \forall (i, j) \in \mathcal{G}(\tau), j' \in [d], \\ x_j - x_{j'} \leq v_{ij} - v_{ij'} \quad \forall (i, j) \in \mathcal{G}(\bar{\tau}), j' \in [d] \end{array} \right\}, \quad (20)$$

which show that they are weighted digraph polyhedra. To ease notation, we introduced the following bi-tropical versions of some familiar objects.

**Definition 17** (Fine-Type Pair and Directed Union). *For any cell  $C$  of  $BCD(V)$ , the fine-type pair matrix  $M(C)$  is a  $n \times d$  matrix formed by*

$$M(C) = M(T, \bar{T}) := T(C, V) - \bar{T}(C, V), \quad (21)$$

where  $T, \bar{T}$  are the fine-type matrices for max- and min-plus respectively. If we also consider their respective covector graphs  $\mathcal{G}_C^{\max}$  and  $\mathcal{G}_C^{\min}$ , we can form what is called their “directed union”  $\mathcal{U}_C$  [14], a  $n \times d$  directed bipartite graph on  $[n] \sqcup [d]$  nodes with arc set

$$\{(i, j) \mid (i, j) \text{ edge of } \mathcal{G}_C^{\max}\} \sqcup \{(j, i) \mid (i, j) \text{ edge of } \mathcal{G}_C^{\min}\}. \quad (22)$$

The following example illustrates these bi-tropical objects.

**Example 3.** Consider the sample  $\mathcal{S} := \{p_1, p_2, p_3, p_4\} = \{(0, 0, 5), (0, 1, 2), (0, 3, 0), (0, 3, 6)\}$  of four points in  $\mathbb{R}^3/\mathbb{R}\mathbf{1}$  and suppose we were to consider a particular cell  $C$  of  $BCD(\mathcal{S})$ , denoted as  $X^E$  in Figure 4. We show the cell's covectors, fine-type pair matrix, and the directed union.

$$V = (v_{ij}) = \begin{bmatrix} 0 & 0 & 0 & 0 \\ 0 & 1 & 3 & 3 \\ 5 & 2 & 0 & 6 \end{bmatrix}^\top, \quad \mathcal{G}_C^{max} = \begin{bmatrix} 0 & 0 & 0 & 0 \\ 1 & 1 & 0 & 1 \\ 0 & 0 & 1 & 0 \end{bmatrix}^\top, \quad \mathcal{G}_C^{min} = \begin{bmatrix} 0 & 1 & 1 & 0 \\ 0 & 0 & 0 & 0 \\ 1 & 0 & 0 & 1 \end{bmatrix}^\top.$$

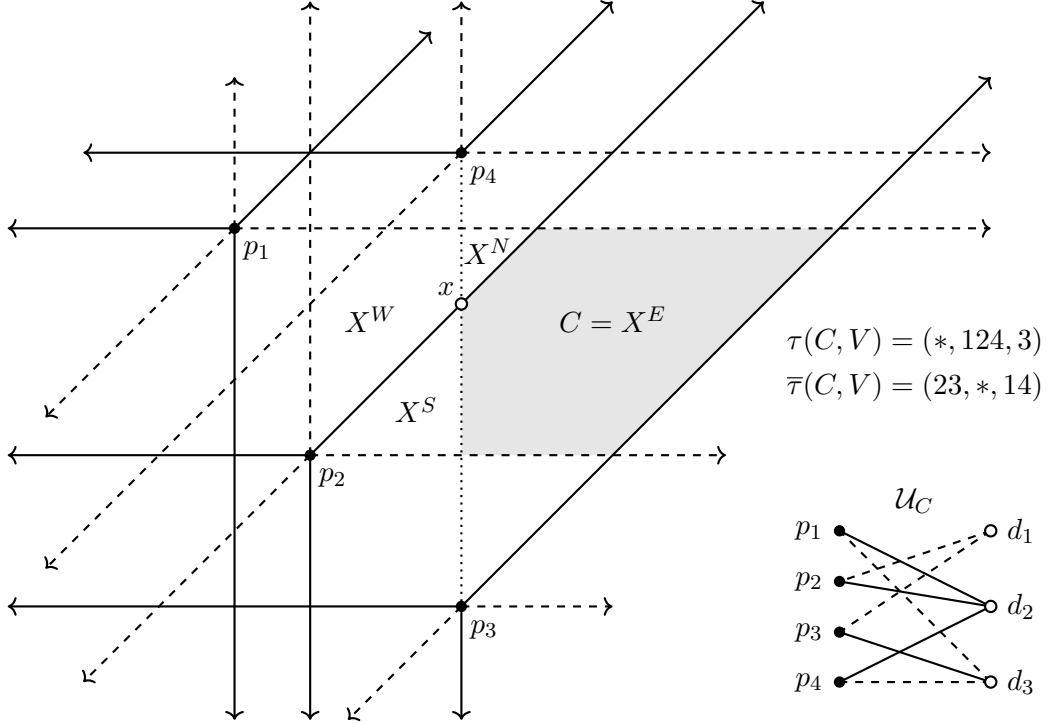


Figure 4: The bi-tropical covector decomposition  $BCD(V)$  of four points in  $\mathbb{R}^3/\mathbb{R}\mathbf{1}$ . Max-plus hyperplanes (solid) and min-plus hyperplanes (dashed) together subdivide the plane. The segment from  $p_3$  to  $p_4$  is dotted to show it corresponds to the overlap of max-plus (from  $p_4$ ) and min-plus (from  $p_3$ ). That is,  $V$  is not in *general position*. The cell  $C$  corresponds to the unique pair of bipartite graphs  $\mathcal{G}_C^{max}$  and  $\mathcal{G}_C^{min}$  which encode the covectors under max-plus/min-plus respectively. Together, they form the directed union graph  $\mathcal{U}_C$  shown to in the bottom-right. The covectors  $\tau(C, V)$  and  $\bar{\tau}(C, V)$  have coarse types  $\#\tau = (0, 3, 1)$  and  $\#\bar{\tau} = (2, 0, 2)$  respectively.

It is important to stress here  $C$  happens to be a maximal cell. As a result, its covector does not contain the covector of any cell of lower dimension contained in  $C$ . For example, the point  $x$  on the boundary of  $C$  is simultaneously its own 0-dimensional cell, a member of each of four 2-dimensional cells ( $X^N, X^E, X^S, X^W$ ), and a member of the four 1-dimensional cells comprising the boundaries between them. The covector graph for  $x$  contains the covector graphs of all higher-dimensional cells containing  $x$ . That is, for two distinct maximal cells  $A$  and  $B$  in  $BCD(V)$ ,

$$x \subseteq \{A \cap B\} \subseteq A \iff \mathcal{U}_x \supseteq \{\mathcal{U}_A \cup \mathcal{U}_B\} \supseteq \mathcal{U}_A. \quad (23)$$

This inclusive/exclusive relationship follows directly from (20). The relationship between cell membership and covector graphs is demonstrated in Figure 5.

### 3 Computing Tropical Fermat-Weber Points

In [17], Lin and Yoshida showed that  $FW(\mathcal{S})$  is a classical polytope in  $\mathbb{R}^d/\mathbb{R}\mathbf{1} \cong \mathbb{R}^{d-1}$  and offered a linear program (LP) with  $FW(\mathcal{S})$  as its optimal solution. We begin this section by briefly revisiting this result and reintroducing the LP. By inspecting the program's dual formulation, we show that  $FW(\mathcal{S})$  is fully characterized as a cell of the sample's bi-tropical covector decomposition  $BCD(\mathcal{S})$ .

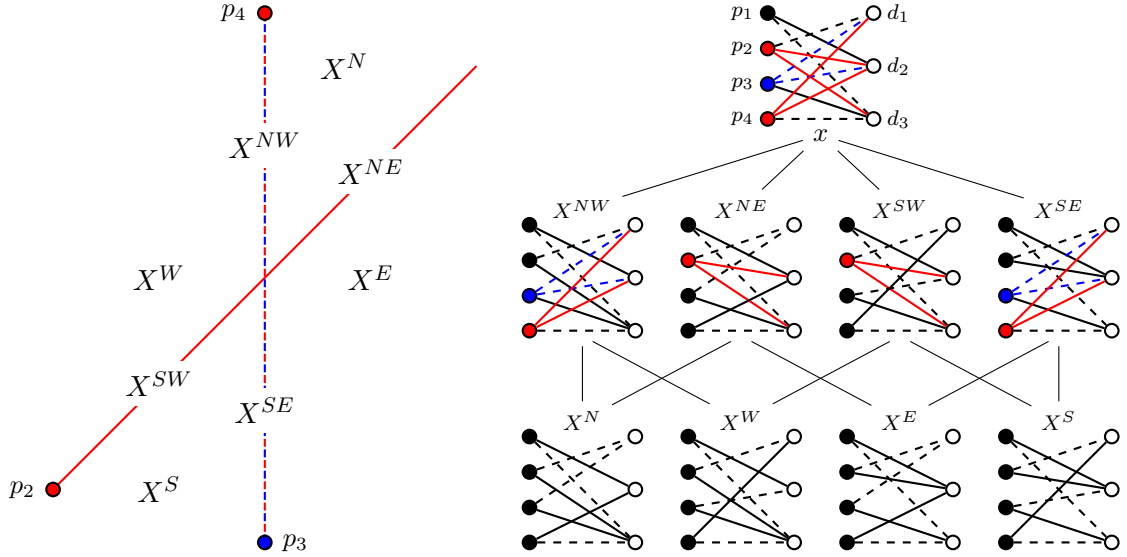


Figure 5: Left: A close-up of Figure 4 for the cells in a neighborhood of  $x$ . Max-plus hyperplanes are colored red, while min-plus hyperplanes are colored blue.  $p_3$  and  $p_4$  are colored to denote their contribution to the corresponding overlapping hyperplanes between them. Right: A lattice of directed unions for all cells in a neighborhood of  $x$  ordered by inclusion from top to bottom. Colored arcs/nodes correspond to arcs not shared by one or more of their children.

### 3.1 The Tropical Fermat-Weber Objective Function

Let us begin by considering the *objective function* introduced via Equation 1, which we will sometimes reference as  $f$ , and whose corresponding objective function value we will refer to as  $Z$ . That is, we have

$$f(x, V) = \sum_{i=1}^n d_{tr}(x, v_i) = \sum_{i=1}^n f_i(x) = Z = z_1 + \dots + z_n, \quad (24)$$

where  $v_i$  are the rows of an  $n \times d$  matrix  $V$  with all finite entries, and  $z_i$  is the tropical distance between  $x$  and  $v_i$ . Recall that a function,  $f : \mathbb{R}^d / \mathbb{R}\mathbf{1} \rightarrow \mathbb{R}$  is convex (in the classic sense) if  $f(\lambda x + (1 - \lambda)y) \leq \lambda f(x) + (1 - \lambda)f(y)$  for any  $x, y \in \mathbb{R}^d / \mathbb{R}\mathbf{1}$  and  $0 \leq \lambda \leq 1$ .

**Lemma 1** (Proposition 6 in [17]).  *$f(x, V)$  is a convex function.*

*Proof.* Consider a single  $f_i(x)$  from (24). We show that  $f_i(x) = d_{tr}(x, p_i) = d_{tr}(\mathbf{0}, p_i - x)$  is a convex function. For  $0 \leq \lambda \leq 1$  and  $x = (x_1, \dots, x_d), y = (y_1, \dots, y_d) \in \mathbb{R}^d / \mathbb{R}\mathbf{1}$ ,

$$\begin{aligned} f_i(\lambda x + (1 - \lambda)y) &= \max_{j \in [d]} (\lambda x_j + (1 - \lambda)y_j) - \min_{j \in [d]} (\lambda x_j + (1 - \lambda)y_j) \\ &\leq \max_{j \in [d]} (\lambda x_j) + \max_{j \in [d]} ((1 - \lambda)y_j) - \min_{j \in [d]} (\lambda x_j) - \min_{j \in [d]} ((1 - \lambda)y_j) \\ &= \lambda f_i(x) + (1 - \lambda)f_i(y). \end{aligned}$$

Thus,  $f_i(x)$  is convex. Since a sum of convex functions is convex, we have the result.  $\square$

Establishing the convexity of  $f(x, V)$  automatically establishes the convexity of  $FW(\mathcal{S})$ , and ensures that any *local minimizer* of  $f(x, V)$  is also a *global minimizer*. Though somewhat obvious, we will call upon these characteristics in the context of a tropical Fermat-Weber gradient.

### 3.2 A Tropical Fermat-Weber Linear Program

The following formulation follows from [17]. Consider a single  $z_i$  where

$$\begin{aligned} z_i &= \max\{v_i - x\} - \min\{v_i - x\} = \max\{v_i - x\} + \max\{-v_i + x\}, \\ z_i &\geq (v_{ij} - x_j) + (-v_{ij'} + x_{j'}) = -x_j + x_{j'} + (v_{ij} - v_{ij'}) \quad \forall j, j' \in [d], \\ z_i + x_j - x_{j'} &\geq v_{ij} - v_{ij'} \quad \forall j, j' \in [d]. \end{aligned}$$

Let  $b_i^{j,j'} = v_{ij} - v_{ij'}$  and note that any case where  $j = j'$  is redundant given  $d_{tr}$  is a metric on  $\mathbb{R}^d/\mathbb{R}\mathbf{1}$ . Thus, we arrive at the following primal formulation:

$$\begin{aligned} \text{(P)} \quad & \text{minimize} \quad \langle \mathbf{1}, \mathbf{z} \rangle + \langle \mathbf{0}, \mathbf{x} \rangle \\ & \text{subject to} \quad z_i + x_j - x_{j'} \geq b_i^{j,j'} \quad \forall (j, j') \in \{[d] \times [d] \mid j \neq j'\}, \quad i = 1, \dots, n \quad [\boldsymbol{\rho}] \end{aligned}$$

to which we associate dual variables  $\rho$ . It is worth noting here that each constraint above describes a Euclidean halfspace, and taken together they describe a weighted digraph polyhedron. They are precisely the union of the max-plus and min-plus envelopes  $\mathcal{E}_{min}(V) \cup \mathcal{E}_{max}$  as described in [14]. The corresponding dual formulation is given by:

$$\begin{aligned} \text{(D)} \quad & \text{maximize} \quad \langle \mathbf{b}, \boldsymbol{\rho} \rangle \\ & \text{subject to} \quad \sum_{1 \leq j < j' \leq d} \rho_i^{j,j'} + \rho_i^{j',j} = 1 \quad i = 1, \dots, n \quad [z] \\ & \quad \quad \quad \sum_{\substack{j' \in [d] \setminus j, \\ i \in [n]}} \rho_i^{j,j'} - \rho_i^{j',j} = 0 \quad j = 1, \dots, d \quad [x] \\ & \quad \quad \quad \boldsymbol{\rho} \geq \mathbf{0}. \end{aligned}$$

From the constraints  $[z]$  and  $[x]$  in (D) we have, by complementary slackness,

$$\left( \sum_{1 \leq j < j' \leq d} (\rho^*)^{j,j'} + (\rho^*)^{j',j} - 1 \right) z_i^* = 0 \quad i = 1, \dots, n, \quad (25)$$

$$\left( \sum_{j' \in [d] \setminus j, i \in [n]} (\rho^*)^{j,j'} - (\rho^*)^{j',j} \right) x_j^* = 0 \quad j = 1, \dots, d. \quad (26)$$

Note that (D) describes a multi-arc, uncapacitated network flow problem for a fully-connected network on  $d$  nodes with no self-loops, with  $\rho_i^{j,j'}$  representing the flow from node  $j$  to node  $j'$  using arc-type  $i$ . This interpretation has several nice features. First, by integrality of the constraints we are guaranteed integer optimal solutions on the flow variables, so that given constraint set  $[z]$  our flows become binary. Second, we can interpret (26) as balance of flow constraints on the node set  $[d]$ , which provide a convenient criterion for testing membership of  $FW(V)$ . Finally, each arc in  $\rho_i$  corresponds to a particular half-sector of  $v_i$ . Together, these imply that our optimal solution  $x^*$  must lie within the intersection of the half-sectors identified by  $\rho^* > 0$ , that is

$$x^* \in \left\{ \bigcap_{(i,j,j')} v_i + \bar{S}^{j,j'} \mid (\rho^*)^{j,j'} > 0 \right\}. \quad (27)$$

An immediate consequence of (27) is that by solving either (P) or (D), one determines the exact selection of half-sectors that define the entire Fermat Weber set. It follows that  $FW(V)$  corresponds exactly with a cell of  $BCD(V)$ . Since all cells in  $BCD(V)$  are polytopes,  $FW(V)$  is as well. We restate this observation now as our main theorem.

**Theorem 1.** *For  $\mathcal{S}$ , a sample of points in  $\mathbb{R}^d/\mathbb{R}\mathbf{1}$ , the Fermat-Weber region  $FW(\mathcal{S})$  is defined by a unique cell in the bi-tropical covector decomposition ( $BCD$ ) induced by  $\mathcal{S}$ . That is,  $FW(\mathcal{S})$  is bi-tropically convex, and is therefore a polytrope.*

*Proof.* By (20), every cell in  $BCD(\mathcal{S})$  is bi-tropically convex. All we must show is that  $FW(\mathcal{S})$  is defined by a unique cell in  $BCD(\mathcal{S})$ . That  $FW(\mathcal{S})$  is a cell of  $BCD(\mathcal{S})$  is a direct result of complementary slackness. That the cell is unique follows from the convexity of the tropical Fermat-Weber distance function  $f$ .  $\square$

**Example 4.** *Let us return to our running example  $V_{4 \times 3}$ . Solutions to (P) or (D) are*

$$\begin{aligned} \{z^*, x^*\} &= \{(4, 0, 4, 4), (0, 1, 2)\}, \\ \{\rho \mid \rho^* = 1\} &= \{\rho_1^{2,3}, \rho_2^{3,1}, \rho_3^{3,2}, \rho_4^{1,3}\}, \\ \langle \mathbf{1}, z^* \rangle + \langle \mathbf{0}, x^* \rangle = \langle \mathbf{b}, \rho^* \rangle &= 12. \end{aligned}$$

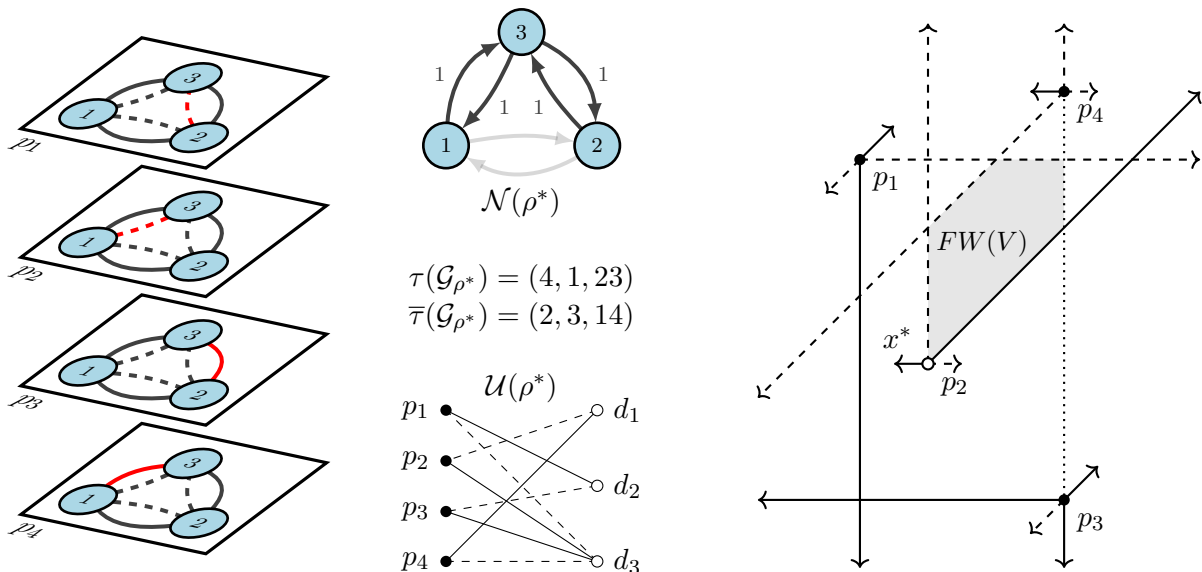


Figure 6: Left: The multi-arc network flow formulation for  $V$  in Example 3. Solid arcs flow in the clockwise direction, while dashed arcs flow counterclockwise. Red arcs indicate the optimal arc selection given by  $\rho^*$ . Center: The network  $\mathcal{N}$  resulting from the summation of arcs given by  $\rho^*$  (top), directed union  $\mathcal{U}(\rho^*)$ (bottom), and corresponding covectors. Within the directed union solid arcs correspond to  $j$  and dashed arcs to  $j'$ . Right: Half-sectors for each point intersect on the shaded region, which corresponds to  $FW(V)$ . Rays corresponding to the max-hyperplane portion of the half-sectors are drawn solid while min-hyperplane portions are dashed.

Figure 6 shows how  $\rho^*$  encodes a set of arcs (one for each point in the sample) within a layered network. These graphs are directed, with solid arcs representing clockwise flow and dashed arcs representing counterclockwise flow. By merging these layers together so that flows combine additively, we get a balanced network on  $[d]$  nodes,  $\mathcal{N}(\rho^*)$ , where each point in  $V$  contributes a single unit of flow. Note how the net flow across each node in  $[d]$  is encoded by the cardinality of the elements of the covectors, i.e. the coarse-types. In the next section we will see in what manner we can leverage these coarse-types to test for optimality conditions indicating whether a particular point is in fact a Fermat-Weber point.

When viewed as half-sectors,  $\rho^*$  defines the set of cones whose intersection contains  $FW(V)$ , as seen on the right of Figure 6. Given  $\rho^*$ , it is a straight-forward exercise to construct the covector graphs and resulting directed union, shown in the center.

Finally, consider that given  $\rho^*$ , max-plus and min-plus types both have, across all indices, unit cardinality (which is by-construction given  $[z]$ ), and that this is equivalent to the statement that their dual coarse-types are both given by the all-ones vector  $(1, \dots, 1)$ . Equivalently, the row sums of the fine-type matrices for both max and min are always one. However, if one were to consider *only* the point  $x^*$  and construct its associated types, covectors, etc. without knowing  $\rho^*$ , the resulting tuples/covectors would have more elements than those constructed via  $\rho^*$ . This is a result of Equation 23, and it means that even if we are luckily enough to select a point in  $FW(V)$  (like  $x^*$ ), the resulting covectors and covector graphs would not necessarily satisfy (26). This issue will come up again in the next section, where we will offer a method of resolution.

## 4 Tropical Fermat-Weber Gradients

The linear program provided in Section 3.2 requires  $nd(d-1)$  constraints and  $n+d$  variables to formulate, and holding such constraints in system memory can become prohibitive when applying this method to real-world datasets. As such, it becomes desirable to have an iterative method, such as gradient descent, that converges to  $FW(\mathcal{S})$ . Leveraging what we now know of the geometric structure of  $FW(\mathcal{S})$ , we propose such a gradient descent scheme that is guaranteed to converge to a Fermat-Weber point.

## 4.1 Gradient for Finding Tropical Fermat-Weber Points

The complementary slackness condition of (25) suggests that the gradients for  $f(x, V)$  can be computed by counting points within a hyperplane arrangement, and that the gradient will only change upon crossing over a hyperplane boundary from one hyperplane sector into another. We will now formalize this intuition.

Let  $C$  be any full-dimensional cell of  $BCD(V)$  with  $x, y$  distinct, arbitrary points in its interior  $\text{int}(C)$ . Define  $\delta := y - x$  and let  $Z = \sum_i z_i = \sum_i d_{tr}(x, v_i)$  be the sum of tropical distances from  $x$  to all points in  $V$ . Similarly, let  $z'_i$  be the corresponding tropical distances from  $y$  to  $v_i$  for all  $i \in [n]$ . Then from (5) we have

$$\begin{aligned} z'_i &= \max\{y - v_i\} - \min\{y - v_i\} = \max\{x + \delta - v_i\} - \min\{x + \delta - v_i\} \\ &= (x_j + \delta_j - v_{ij}) - (x_{j'} + \delta_{j'} - v_{ij'}) \\ &= z_i + \delta_j - \delta_{j'}, \end{aligned} \quad (28)$$

where the last two equalities hold since by definition of covectors, the maximal and minimal indices of  $(x - v_i)$  do not vary for any  $x \in \text{int}(C)$ . Then for  $Z' = \sum_i d_{tr}(y, v_i)$  we have

$$\begin{aligned} Z' = \sum_i z'_i &= \sum_i z_i + \sum_{j=1}^d \sum_{k \in \tau_k(y)} \delta_k - \sum_{j=1}^d \sum_{k \in \bar{\tau}_k(y)} \delta_k \\ &= Z + \sum_{j=1}^d (\#\tau_j(y))\delta_j - \sum_{j=1}^d (\#\bar{\tau}_j(y))\delta_j \\ &= Z + \langle \#\tau(y), \delta \rangle - \langle \#\bar{\tau}(y), \delta \rangle. \\ Z' &= Z + \langle \#\tau(y) - \#\bar{\tau}(y), \delta \rangle. \end{aligned}$$

Thus, as  $\delta \rightarrow \mathbf{0}$ , we have

$$\nabla f(x, V) = \lim_{\delta \rightarrow \mathbf{0}} \frac{Z' - Z}{\|\delta\|} = \lim_{\delta \rightarrow \mathbf{0}} \frac{\langle \#\tau(y) - \#\bar{\tau}(y), \delta \rangle}{\|\delta\|} = \#\tau(y) - \#\bar{\tau}(y). \quad (29)$$

This derivation shows explicitly that the gradient of  $f(x, V)$  is defined by the difference in max-plus and min-plus coarse-types. That is, the gradient is the course-type (column sums) of the directed union  $\mathcal{U}_C$  as defined in (22).

**Definition 18** (Tropical Fermat-Weber Gradient). *Let  $V$  be a  $n \times d$  matrix with finite coefficients. For any full-dimensional cell  $C$  in  $BCD(V)$ , the tropical Fermat-Weber gradient of its interior is the difference between the max-plus and min-plus coarse-types of cell  $C$ . That is,*

$$\nabla f(C, V) := \#\tau(C, V) - \#\bar{\tau}(C, V). \quad (30)$$

For cells of maximal dimension, a tropical Fermat-Weber gradient is well-defined, as both covectors  $\tau$  and  $\bar{\tau}$  are uniquely determined. However, as we have already seen, nested cells of lower dimension have covectors that contain the covectors of all higher-dimensional cells to which they belong. Thus, when applying Equation (28) for such lower-dimensional cells it is unclear which indices  $j, j'$  to select given ties in the data. To handle such instances of non-differentiability, we develop the notion of subgradients for cells that are not maximal, i.e., for points along the boundary of full-dimensional cells as follows.

**Definition 19** (Tropical Fermat-Weber Subdifferential). *Given a set of points  $v_i \in \mathbb{R}^d/\mathbb{R}\mathbf{1}$  for  $i \in [n]$ , the tropical Fermat-Weber subdifferential of a point  $x \in \mathbb{R}^d/\mathbb{R}\mathbf{1}$  is the cone generated by the tropical Fermat-Weber gradients of all maximal covector cells in an open neighborhood of  $x$ .*

**Lemma 2.** *Any tropical Fermat-Weber subgradient is an element of the subdifferential of  $f(x, V)$ .*

*Proof.* Consider a case in which for some  $x \in \mathbb{R}^d/\mathbb{R}\mathbf{1}$  and for some  $v_k \in V$  we have the maximum of  $x - v_k$  achieved at least twice and/or the minimum of  $x - v_k$  achieved at least twice. Let  $\{i'\}$  denote the set of indices that achieve the maximum, and  $\{j'\}$  the set that achieves the minimum. Note that it is possible that  $\{i'\} = \{j'\} = [d]$  if  $x = v_k$ . For any selection  $(i \in \{i'\}, j \in \{j'\})$  with  $i \neq j$ , take  $e_i - e_j$  as the corresponding unit-vector direction. With this selection of  $i$  and  $j$  the gradient in (28) becomes well-defined, and we denote it as  $\Delta_{ij}$ . Now, consider some small  $\epsilon > 0$ . We perturb the point  $x$  according to  $x' = x + (e_i - e_j)\epsilon$  and note that

$$f(x', V) \geq f(x, V) + \Delta_{ij}^\top (x' - x), \quad (31)$$

which satisfies the supporting hyperplane condition. Note that if  $x'$  is in the interior of a cell of maximal dimension, then by construction  $\nabla f(x', V) = \Delta_{ij}$ . Since  $i, j$  were arbitrary, this condition holds over all  $i \neq j$ , meaning that any gradient of a maximal cell in a neighborhood of  $x$  will also satisfy the supporting hyperplane condition. That is to say, the subgradient of Definition 19 satisfies this condition.  $\square$

Let's demonstrate the gradient and subgradient calculations with an example. We continue with  $V$  from Example 3 and consider the point  $x = (0, 3, 4)$  shown in Figure 4 and Figure 7. Here,  $x$  is adjacent to four maximal cells, which we identify as  $X^N, X^E, X^S$ , and  $X^W$  based on their general cardinal direction from  $x$ . For each of these maximal cells we calculate the gradient, using  $X^S$  to demonstrate.

**Example 5.** Select  $y \in \text{int}(X^S)$  and for each  $v_i \in V$  calculate  $\text{argmax}\{y - v_i\}$  and  $\text{argmin}\{y - v_i\}$ . Per Equation 10, one can equivalently calculate covectors by considering the arrangement of min/max-plus tropical hyperplanes with apices at  $y$  and noting which points in  $\mathcal{S}$  are contained in  $y + S^{\text{min},j}$  and  $y + S^{\text{max},j}$  for  $j \in [d]$ . This "swapping" allows us to draw a somewhat less cluttered Figure 7 in that we need only add a single pair of hyperplanes at  $y$  vice the full decomposition of Figure 4. Since our usual convention in this paper is to draw max-plus hyperplanes solid and min-plus hyperplanes dashed, we apply the reverse convention at  $y$  to remind the reader we have "swapped." With  $y = (0, 2.5, 2.6)$  and  $p_1$  we get  $\text{argmax}\{p_1 - y\} = \text{argmax}\{0, 2.5, -2.4\} = 2$  and  $\text{argmin}\{0, 2.5, -2.4\} = 3$ . Repeating this for  $p_2, p_3, p_4$  we get the covectors shown in Figure 7.

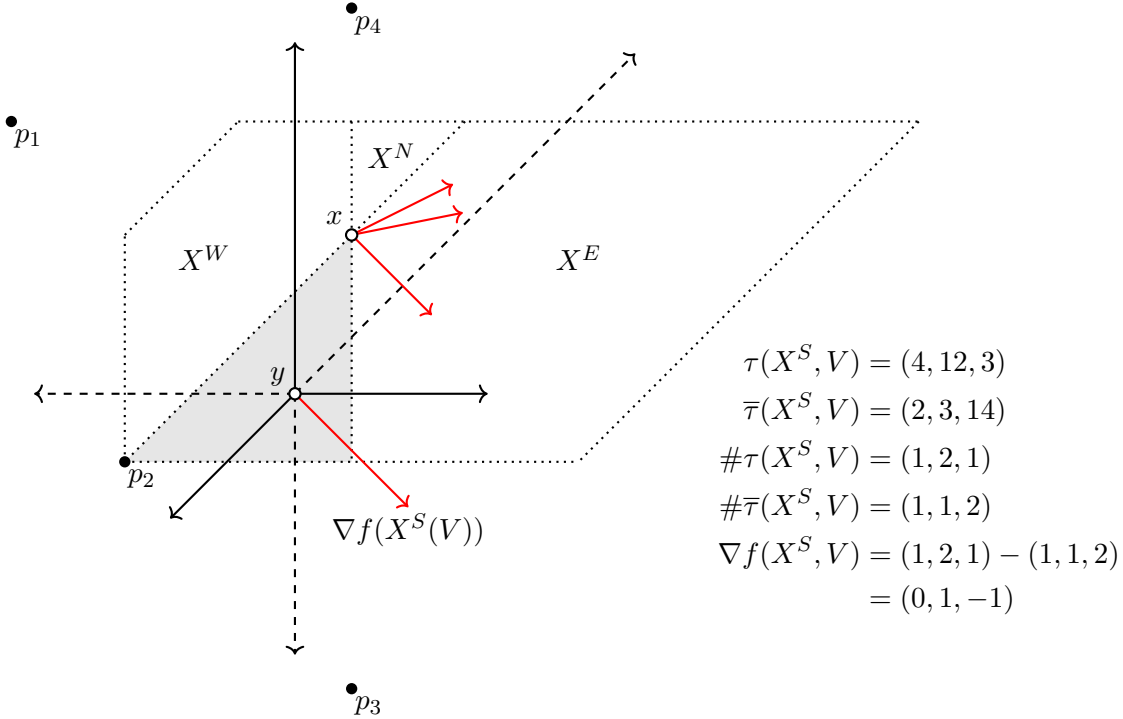


Figure 7: A portion of  $BCD(V)$  comprising the full-dimensional cells (dotted) containing  $x$ . For  $y \in \text{int}(X^S)$  (shaded gray) the gradient (in red) amounts to counting points within the sectors of  $\mathcal{F}(y)$ . The subdifferential evaluated at  $x$  is seen by the cone formed from the set of all tropical gradients of full-dimensional cells in an open neighborhood of  $x$  (also in red).

Repeating these steps for the other maximal cells yields:

$$\begin{aligned} \nabla f(X^N, V) &= \#(*, 14, 23) - \#(23, *, 14) = (0, 2, 2) - (2, 0, 2) = (-2, 2, 0) \mapsto (0, 4, 2) \\ \nabla f(X^E, V) &= \#(*, 124, 3) - \#(23, *, 14) = (0, 3, 1) - (2, 0, 2) = (-2, 3, -1) \mapsto (0, 5, 1) \\ \nabla f(X^W, V) &= \#(4, 1, 23) - \#(2, 3, 14) = (1, 1, 2) - (1, 1, 2) = (0, 0, 0). \end{aligned}$$

With all gradients in hand, the tropical subdifferential at  $x$  is

$$\frac{\partial f(x, V)}{\partial x} = \text{tpos} \left\{ \begin{pmatrix} 0 \\ 4 \\ 2 \end{pmatrix}, \begin{pmatrix} 0 \\ 5 \\ 1 \end{pmatrix}, \begin{pmatrix} 0 \\ 1 \\ -1 \end{pmatrix}, \begin{pmatrix} 0 \\ 0 \\ 0 \end{pmatrix} \right\}.$$

In this example, the fact that zero is an element of the subdifferential evaluated at  $x$  indicates that  $x$  is a tropical Fermat-Weber point of  $V$ . Perhaps more significant, however, is the fact that  $\nabla f(X^W, V) = \mathbf{0}$ , i.e.,  $X^W$  has *zero-gradient*. In fact, the cell  $X^W$  is precisely the Fermat-Weber set. That this zero-gradient condition is necessary and sufficient for  $FW(V)$  follows directly from complementary slackness.

It should be clear from the definition of the gradient that  $\nabla f(C, V) = 0 \iff \#\tau(C, V) = \#\bar{\tau}(C, V)$ , that is, the maximal and minimal coarse-types must *balance*. We will refer to this condition as the *balancing condition* for tropical Fermat-Weber gradients. The balancing condition implies that for any point  $x \in FW(V)$ , and for every dimension  $j \in [d]$ , the number of points  $v_i \in V$  with  $\operatorname{argmax}\{x - v_i\} = j$  equals the number of points with  $\operatorname{argmin}\{x - v_i\} = j$ .

## 4.2 A Tropical Fermat-Weber Gradient Descent Algorithm

Following our definitions above, we propose a gradient descent algorithm for the tropical Fermat-Weber region as follows. To begin, we first need a rule for selecting a subgradient from the subdifferential of any point not in the interior of a maximal cell of  $BCD(V)$ . One straightforward method might be to simply average the generators defining the cone of the subdifferential. For  $x$  from Example 3, that would look like

$$\widehat{\nabla}(f(x, V)) = \frac{1}{4} \left[ \begin{pmatrix} 0 \\ 4 \\ 2 \end{pmatrix} + \begin{pmatrix} 0 \\ 5 \\ 1 \end{pmatrix} + \begin{pmatrix} 0 \\ 1 \\ -1 \end{pmatrix} + \begin{pmatrix} 0 \\ 0 \\ 0 \end{pmatrix} \right] = \begin{pmatrix} 0 \\ 5/2 \\ 1/2 \end{pmatrix} \in \frac{\partial f(x, V)}{\partial x}.$$

Another method might consider applying weights to each covector's elements according to some scheme, such as uniform, applied to the fine-type matrices. For example, suppose a particular  $\max\{p_i - x\}$  has  $m > 1$  maximal elements. Then, before taking column sums during coarse-type calculations, normalize the  $i$ -th row of  $T(p_i - x, V)$  by dividing it by  $m$ , and do this for all points in both max and min conventions. For  $x$  in Example 3, this would look like

$$T = \begin{bmatrix} 0 & 0 & 0 & 1 \\ 1 & 1 & 0 & 1 \\ 0 & 1 & 1 & 0 \end{bmatrix}^\top \rightarrow \begin{bmatrix} 0 & 0 & 0 & 1/2 \\ 1 & 1/2 & 0 & 1/2 \\ 0 & 1/2 & 1 & 0 \end{bmatrix}^\top, \quad \bar{T} = \begin{bmatrix} 0 & 1 & 1 & 0 \\ 0 & 0 & 1 & 0 \\ 1 & 0 & 0 & 1 \end{bmatrix}^\top \rightarrow \begin{bmatrix} 0 & 1 & 1/2 & 0 \\ 0 & 0 & 1/2 & 0 \\ 1 & 0 & 0 & 1 \end{bmatrix}^\top,$$

$$\widehat{\nabla}(f(x, V)) = \begin{pmatrix} 0.5 \\ 2 \\ 1.5 \end{pmatrix} - \begin{pmatrix} 1.5 \\ 0.5 \\ 2 \end{pmatrix} = \begin{pmatrix} -1 \\ 1.5 \\ -1.5 \end{pmatrix} \mapsto \begin{pmatrix} 0 \\ 5/2 \\ 3/2 \end{pmatrix} \in \frac{\partial f(x, V)}{\partial x}. \quad (32)$$

This second method has a computational advantage in that we are not required to enumerate covectors across all maximal cells adjacent to  $x$ . Yet both methods critically miss that  $x \in FW(V)$ , that is, we want a method that can *detect* if  $\mathbf{0}$  is in the subdifferential. We now propose such a method, where the main idea rests on the sufficiency of the *balancing condition*.

**Lemma 3.** *For any point  $x \in \mathbb{R}^d/\mathbb{R}\mathbf{1}$ ,  $x$  satisfies the balance condition (and is therefore a Fermat-Weber point) if and only if there exists a subset of its directed union such that the in-degree and out-degree for each node  $j \in [d]$  are equal and  $i \in [n]$  has no isolated nodes.*

*Proof.* That the in-degree equals the out-degree for every node  $j \in [d]$  is a direct result of the complementary slackness conditions associated with  $[x]$ . Similarly, that there can be no isolated nodes for  $i \in [n]$  follows from the complementary slackness conditions associated with  $[z]$ .  $\square$

Suppose we construct a directed graph with  $2n + d$  nodes in the following way. From  $K_{n,d}$ , split all nodes in the set  $[n]$  into two separate sets, one pertaining to a max-plus version ( $u_i$ ) and one to a min-plus version ( $v_i$ ). Note that we now have a  $\{[u] \cup [v]\} \sqcup [d]$  graph that is still bipartite. Make all arcs directed so that nodes in  $[u]$  go to  $[d]$ , nodes in  $[d]$  go to  $[v]$ , and assign all of them zero capacity. Now, add special  $s$  and  $t$  nodes and arcs to form a maximum circulation network. Specifically, add arcs  $(s, u_i)$  and  $(v_i, t)$  for  $i \in [n]$  with unit capacity, and an uncapacitated arc  $(t, s)$ . We call the resulting network  $\Gamma$ , noting that it has  $2n + d + 2$  nodes and  $2n(d + 1) + 1$  arcs, which we denote  $(\mathcal{A})$ . See Figure 8 for an example.

We propose to run a maximum network flow algorithm over this graph given a particular point  $x$  to determine if zero is in its subdifferential. To do so, we update  $\Gamma$  based on  $x$  in the following way. Consider  $\mathcal{U}(x, V)$ , the directed union at  $x$ . For every (solid) max-plus arc  $(i, j)$  in  $\mathcal{U}(x, V)$ , update the capacity of arc  $(u_i, d_j)$  in  $\mathcal{A}$  to one. Similarly, for every (dashed) min-plus arc  $(i, j)$ , update the capacity of  $(d_j, v_i)$  in  $\mathcal{A}$  to one. This network flow problem has  $2n + d + 2$  flow-balance

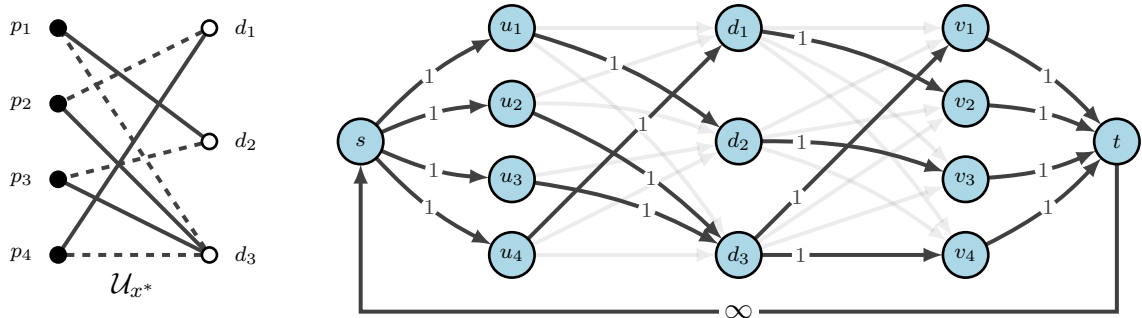


Figure 8: The directed union graph (left) from Example 3 for the point  $x^* = (0, 2, 1)$  and the network  $\Gamma(x)$  generated by splitting its nodes into two sets (right). Solid arcs have unit capacity except  $(t, s)$  which is uncapacitated. Zero-capacity arcs from  $\Gamma$  are shown in light grey. A max flow solution on  $\Gamma(x)$  yields an objective value  $\gamma^* = n$  if and only if  $x^*$  is a Fermat-Weber point.

constraints and  $2n(d+1) + 1$  capacity constraints, far fewer than the  $nd(d-1)$  constraints from  $(\mathbf{P})$  when  $d$  becomes large.

By construction, the max possible flow over  $\Gamma(x)$  can never exceed  $n$ , and in particular, achieving this maximum requires two conditions. First, that every node  $u_i \in \{u\}$  (resp.  $v_i \in \{v\}$ ) has one unit of flow across it, and second, that all nodes in  $[d]$  achieve flow balance. These somewhat obvious conditions are stated here to reinforce their connection to the earlier constraints in  $(\mathbf{D})$  and to Lemma 3. The maximum flow value  $\gamma^*(x)$  on  $\Gamma(x)$  tells us precisely if a zero subgradient exists within the subdifferential of a non-interior point  $x$ . When a zero subgradient exists, the optimal flow  $\gamma^*(x)$  recovers  $\rho^*$  from  $(\mathbf{D})$  by considering arcs incident to  $[d]$  with positive flow. Unfortunately, for solutions where  $\gamma^*(x) < n$ , the resultant flows do not generally correspond to gradients. When this happens we simply utilize one of the previous subgradient selection methods.

By constructing  $\Gamma(x)$  we possess at a polynomial time method of checking the zero-gradient condition for a point  $x$  in a non-maximal cell of  $BCD(V)$ . We are now ready to present our gradient descent algorithm.

---

### Algorithm 1 Tropical Fermat-Weber Gradient Descent

---

**Input:** Sample  $V_{n \times d}$  of  $n$  points in  $\mathbb{R}^d / \mathbb{R}\mathbf{1}$ ,  $x^0$  a starting point, and  $\alpha$  step size.

**Output:**  $x^* \in FW(V)$  a tropical Fermat-Weber point and  $\rho^*$  the set of half-sectors defining  $FW(V)$

Generate  $\Gamma$  with arc set  $\mathcal{A}$

**while**  $\widehat{\nabla}(f(x^k, V)) \neq \mathbf{0}$  **do**

    Compute  $T(x^k, V)$  and  $\bar{T}(x^k, V)$  (Equation 12)

**if**  $\max\{\#\tau(x^k, V), \#\bar{\tau}(x^k, V)\} > 1$  **then**

        Update  $\mathcal{A}$ , run max-flow over  $\Gamma(x^k)$  to get  $\gamma^*(x^k)$

**if**  $\gamma^*(x^k) = n$  **then stop**

**else** Compute  $\widehat{\nabla}(f(x^k, V))$  (Equation 32)

**else** Compute  $\widehat{\nabla}(f(x^k, V))$  (Equation 30)

    Update  $x^{k+1} = x^k - \alpha_k \widehat{\nabla}(f(x^k, V))$

---

## 5 Discussion

In this paper we show that the set of all tropical Fermat-Weber points with respect to  $d_{\text{tr}}$  forms a polytrope, a bounded cell of the union of max-plus and min-plus covector decompositions generated by max- and min-plus tropical hyperplane arrangements defined by the set of tropical hyperplanes with apices  $\mathcal{S} = \{p_1, \dots, p_n\}$ . This cell, which may not be full-dimensional, has the property that, for some subset of its directed union graph, the associated dual coarse-types balance across every dimension. This insight enabled us to construct a network flow problem that can check for the zero-gradient condition in polynomial time, and additionally, a gradient descent algorithm with provable convergence that requires significantly less overhead memory requirements than the linear programming formulation originally proposed in [17].

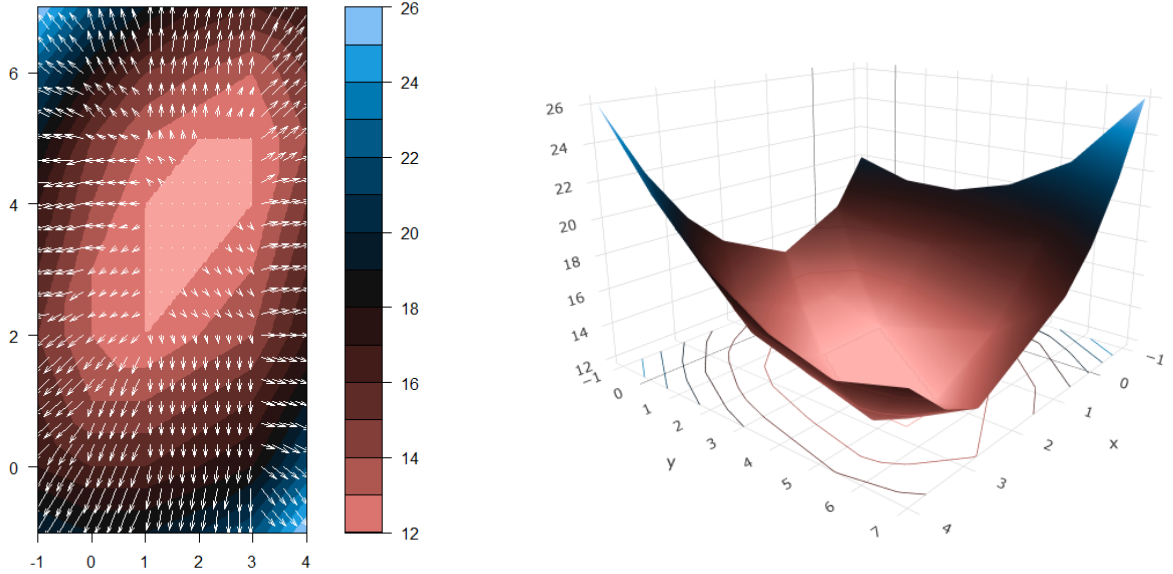


Figure 9: On the left, a contour plot of  $f(x, V)$  for  $V$  given as in Example 3 and centered on the cell  $X^W$ . The arrows are the tropical Fermat-Weber gradients for various locations  $x$  in the proximity of  $X^W$ . On the right, a three-dimensional rendering of  $f(x, V)$  over the same region.

Throughout we only considered samples with uniform weighting on the points, which is to say we considered an *unweighted* Fermat-Weber calculation. Recently Cox and Curiel studied positively-weighted tropical Fermat-Weber points in [7] using the *asymmetric tropical metric*, showing that the set of all weighted tropical Fermat-Weber points with respect to the asymmetric tropical metric forms a tropical polytope. Future research should investigate the geometry of the set of all positively-weighted tropical Fermat-Weber points with respect to the symmetric tropical metric  $d_{\text{tr}}$ , namely: a weighted tropical Fermat-Weber point of a sample  $\mathcal{S} = \{p_1, \dots, p_n\} \subset \mathbb{R}^d/\mathbb{R}\mathbf{1}$  defined as

$$x^* = \arg \min_x \sum_{i=1}^n \alpha_i d_{\text{tr}}(x, p_i)$$

where  $0 \leq \alpha_i \leq 1$  for  $i = 1, \dots, n$  and  $\sum_{i=1}^n \alpha_i = 1$ . One can easily show that the set of all weighted tropical Fermat-Weber points with respect to the symmetric tropical metric  $d_{\text{tr}}$  of a given sample  $\mathcal{S} \subset \mathbb{R}^d/\mathbb{R}\mathbf{1}$  forms a classical convex polytope in  $\mathbb{R}^{d-1} \cong \mathbb{R}^d/\mathbb{R}\mathbf{1}$  by Lemma 1. Here we have the following conjecture:

**Conjecture 1.** *Suppose we have a sample  $\mathcal{S} = \{p_1, \dots, p_n\} \subset \mathbb{R}^d/\mathbb{R}\mathbf{1}$ . Then the set*

$$WFW(\mathcal{S}) := \left\{ x^* \in \mathbb{R}^d/\mathbb{R}\mathbf{1} \mid x^* = \arg \min_x \sum_{i=1}^n \alpha_i d_{\text{tr}}(x, p_i), 0 \leq \alpha_i, \text{ for } i \in [n], \sum_{i=1}^n \alpha_i = 1 \right\}$$

*forms a polytope in  $\mathbb{R}^{d-1} \cong \mathbb{R}^d/\mathbb{R}\mathbf{1}$ .*

Given the interest in applying symmetric Fermat-Weber points to various areas in phylogenetics, it is natural to consider how methods proposed here might apply to datasets possessing a particular structure, e.g., that of coalescent trees. Such trees can be defined on a finite metric space with  $[m] := \{1, \dots, m\}$  and represented by a nonnegative symmetric  $m \times m$ -matrix  $D = (d_{ij})$  with zero entries on the diagonal such that all triangle inequalities are satisfied:

$$d_{ik} \leq d_{ij} + d_{jk} \quad \text{for all } i, j, k \text{ in } [m] := \{1, 2, \dots, m\}.$$

If we consider strengthening these inequalities to:

$$d_{ik} \leq \max(d_{ij}, d_{jk}) \quad \text{for all } i, j, k \in [m],$$

then the metric  $D$  is called an *ultrametric*. The set of all ultrametrics contains the ray  $\mathbb{R}_{\geq 0}\mathbf{1}$  spanned by the all-one metric  $\mathbf{1}$ , which is defined by  $d_{ij} = 1$  for  $1 \leq i < j \leq m$ . The image of the set of ultrametrics, denoted as  $\mathcal{U}_m$ , in the quotient space  $\mathbb{R}^{\binom{[m]}{2}}/\mathbb{R}\mathbf{1}$  is called the *space of ultrametrics*. It is well known that  $\mathcal{U}_m$  is the support of a pointed simplicial fan of dimension  $m-2$  [3, 18, 11, 19].

Lin et al. in [16] showed that even if  $\mathcal{S} = \{p_1, \dots, p_n\} \subset \mathcal{U}_m$ ,  $FW(\mathcal{S}) \not\subset \mathcal{U}_m$ . Aliatimis et al. in [1] showed that a Fermat-Weber point in  $FW(\mathcal{S}) \cap \mathcal{U}_m$  is an estimated species tree from the set of gene trees  $\mathcal{S} = \{p_1, \dots, p_n\} \subset \mathcal{U}_m$  under their proposed model with the tropical metric. Therefore it is one of our interests to study geometry and combinatorics of  $FW(\mathcal{S}) \cap \mathcal{U}_m$ .

## Acknowledgement

RY, DB, and JS are partially supported from NSF DMS 1916037 and 2409819. Part of this research was performed while DB was visiting the Institute for Mathematical and Statistical Innovation (IMSI), which is supported by the National Science Foundation (Grant No. DMS-1929348). KM is partially supported by JSPS KAKENHI Grant Numbers JP22K19816 and JP22H02364.

## References

- [1] G. Aliatimis, R. Yoshida, B. Boyacı, and J. Grants. Tropical logistic regression model on space of phylogenetic trees. *Bull Math Biol*, 86(99), 2024. doi: <https://doi.org/10.1007/s11538-024-01327-8>.
- [2] F. Ardila and M. Develin. Tropical hyperplane arrangements and oriented matroids. *Math. Z.*, 262:795–816, 2009. <https://doi.org/10.1007/s00209-008-0400-z>.
- [3] F. Ardila and C. J. Klivans. The bergman complex of a matroid and phylogenetic trees. *journal of combinatorial theory. Series B*, 96(1):38–49, 2006.
- [4] J. Brimberg. The fermat—weber location problem revisited. *Mathematical Programming*, 71: 71–76, 1995.
- [5] Andrei Comănesci. Tropical convexity in location problems. *Math Meth Oper Res*, 100:509–534, 2024.
- [6] Andrei Comănesci and Michael Joswig. Tropical medians by transportation. *Mathematical Programming*, 205(1–2):813–839, July 2023. ISSN 1436-4646. doi: 10.1007/s10107-023-01996-8. URL <http://dx.doi.org/10.1007/s10107-023-01996-8>.
- [7] Shelby Cox and Mark Curiel. The tropical polytope is the set of all weighted tropical fermat-weber points, 2023. available at <https://arxiv.org/abs/2310.07732>.
- [8] F. Criado, M. Joswig, and F. Santos. Tropical bisectors and voronoi diagrams. *Found Comput Math*, 22:1923–1960, 2022. <https://doi.org/10.1007/s10208-021-09538-4>.
- [9] M. Develin and B. Sturmfels. Tropical convexity. *Documenta Math.*, 9:1–27, 2004.
- [10] Anton Dochtermann, Michael Joswig, and Raman Sanyal. Tropical types and associated 10563 cellular resolutions. *J. Algebra*, 356:304–324, 2012.
- [11] A. Gavruskin and A. Drummond. The space of ultrametric phylogenetic trees. *Journal of Theoretical Biology*, 403:197–208, 2016.
- [12] P. M. Huggins, W. Li, D. Haws, T. Friedrich, J. Liu, and R. Yoshida. Bayes Estimators for Phylogenetic Reconstruction. *Systematic Biology*, 60(4):528–540, 04 2011. ISSN 1063-5157. doi: 10.1093/sysbio/syr021. URL <https://doi.org/10.1093/sysbio/syr021>.
- [13] M. Joswig. Tropical halfspaces. *Combinatorial and computational geometry*, 52(1):409–431, 2005.
- [14] Michael Joswig. *Essentials of Tropical Combinatorics*. Springer, New York, NY, 2021.
- [15] Michael Joswig and Katja Kulas. Tropical and ordinary convexity combined. *Advances in Geometry*, 10(2):333–352, 2010. doi: doi:10.1515/advgeom.2010.012. URL <https://doi.org/10.1515/advgeom.2010.012>.

- [16] B. Lin, B. Sturmfels, X. Tang, and R. Yoshida. Convexity in tree spaces. *SIAM Discrete Math*, 3:2015–2038, 2017.
- [17] Bo Lin and Ruriko Yoshida. Tropical fermat-weber points. *SIAM J. Discret. Math.*, 32:1229–1245, 2018. URL <https://api.semanticscholar.org/CorpusID:51877135>.
- [18] D. Maclagan and B. Sturmfels. *Introduction to Tropical Geometry*, volume 161 of *Graduate Studies in Mathematics*. Graduate Studies in Mathematics, 161, American Mathematical Society, Providence, RI, 2015.
- [19] D. Speyer and B. Sturmfels. Tropical mathematics. *Mathematics Magazine*, 82:163–173, 2009.
- [20] E. Weiszfeld. Sur le point par lequel la somme des distances de n points donnés est minimum. *Tohoku Mathematics Journal*, 43:355–386, 1937.
- [21] Günter M. Ziegler. *Fans, Arrangements, Zonotopes, and Tilings*, pages 191–230. Springer New York, New York, NY, 1995. ISBN 978-1-4613-8431-1. doi: 10.1007/978-1-4613-8431-1\_7. URL [https://doi.org/10.1007/978-1-4613-8431-1\\_7](https://doi.org/10.1007/978-1-4613-8431-1_7).